



Please send any comments, feedback, or suggestions to  
[benjamin.hatchett@colostate.edu](mailto:benjamin.hatchett@colostate.edu)

This is a non-peer-reviewed preprint submitted to EarthArXiv.

This Work has not yet been peer-reviewed and is provided by the contributing Author(s) as a means to ensure timely dissemination of scholarly and technical Work on a noncommercial basis. Copyright and all rights therein are maintained by the Author(s) and may be transferred without further notice. It is understood that all persons copying this information will adhere to the terms and constraints invoked by each Author's copyright. This Work may not be reposted without explicit permission of the copyright owner.

1 Highlights

2 **Revisiting Pyroclimographs\***

3 Benjamin J. Hatchett, T. Todd Lindley

- 4     • Pyroclimographs use daily satellite fire detections to indicate the sea-  
5       sonality of wildland fire activity.
- 6     • Examples across fire-prone regions demonstrate potential use cases and  
7       applications of pyroclimographs.
- 8     • Incorporating additional fire environment data highlights how fire weather  
9       deviates from climatology.

10

# Revisiting Pyroclimographs

11

Benjamin J. Hatchett<sup>a,b</sup>, T. Todd Lindley<sup>c</sup>

<sup>a</sup>*Cooperative Institute for Research in the Atmosphere, Colorado State University, 3925a  
Laporte Ave, Ft. Collins, Colorado, 80521, United States of America*

<sup>b</sup>*Corrspondence to: benjamin.hatchett@colostate.edu,*

<sup>c</sup>*National Weather Service, 120 David L. Boren Blvd., Suite  
2400, Norman, Oklahoma, 73072, United States of America*

---

## 12 Abstract

Wildland fire activity often demonstrates distinct seasonality. Multiple peaks of activity may occur throughout the year with varying magnitudes and durations due to climatologically conducive conditions for wildfire activity or intentional burning. However, anomalous fire environment conditions may favor out-of-season wildfires. Characterization of conditions that increase fire ignition probabilities, extreme fire behavior, and beneficial fire potential enhances our understanding of fire history and past fire behavior while providing insight into how forecast conditions may influence subsequent wildland fires. Here, we apply a commonly-utilized approach to display a region's temperature and precipitation climatology—the climograph—to visually communicate the seasonal cycle, interannual variability, and individual wildland fire events at daily resolution using period-of-record satellite observations from the Moderate Resolution Imaging Spectroradiometer. Counts of detections and cumulative fire radiative power provide first-order indicators of elevated or reduced fire activity, either typically (i.e., wildfire season or prescribed burning season) or anomalously (i.e., out-of-season wildfire). Using a case study of Southern California, we show how pyroclimograph results vary as the region of interest shifts and how their interpretation can be complemented with additional fire environment data.

13

*Keywords:* climatology, fire weather, remote sensing, visualization,

14

wildland fire

---

\*This is a working paper that has not undergone independent peer review.

## 15 1. Introduction

16 Climographs display the monthly mean temperature range and total pre-  
17 cipitation of a location or region (e.g., Lasantha et al., 2022; Al-Yaari et al.,  
18 2023). Just as the climate of a region demonstrates a seasonal cycle, many  
19 regions also demonstrate a seasonal cycle of fire activity (Swetnam et al.,  
20 2011; Al-Yaari et al., 2023; Senande-Rivera et al., 2022). This seasonality re-  
21 sults from both the annual march of plant phenology (i.e., a growing season  
22 when fuel accumulates and a dormant season when fuel becomes available for  
23 combustion) and short- and long-term weather conditions including the on-  
24 set and termination of seasonal drought, ignition sources from lightning, and  
25 otherwise hot, dry, and windy conditions amidst receptive fuelbeds (Dennison  
26 and Moritz, 2009).

27 Linking climatic conditions to the annual cycle of fire activity was first  
28 proposed by (Swetnam et al., 2011), who termed the juxtaposition of monthly  
29 mean temperature and precipitation with monthly burned area a ‘pyroclimo-  
30 graph’. Sablan et al. (2024) developed similar visualizations of monthly fire  
31 activity to show the mean, top and bottom 10<sup>th</sup> percentiles as well as high-  
32 light a year of interest (c.f. their Figure 3b). Sweeney et al. (2025) gen-  
33 erated weekly-timescale visualizations and separated prescribed burns (pile  
34 and broadcast) from wildfires to show the distinct seasonalities of wildland  
35 fire types. However, wildland fires do not always occur on monthly or weekly  
36 timescales, nor do they always occur during climatologically-mean condi-  
37 tions. This implies a monthly–weekly temporal aggregations are potentially  
38 less useful to indicate why normal or anomalous fire activity occurs. Further,  
39 temporal aggregation limits our interpretation of how anomalous the environ-  
40 mental conditions were compared to climatology when fire activity increases.  
41 Establishing a detailed understanding of the conditions that lead to increased  
42 receptiveness of fuels and the potential for extreme fire behavior at ignition-  
43 and fuel receptiveness-relevant timescales may support fire management and  
44 community adaptation efforts at longer timescales (i.e., annual to decadal) as  
45 well as characterizing a region’s general fire environment. This is especially  
46 true when identifying conditions to safely and effectively conduct prescribed  
47 burning (Worsnop et al., in revision; Hatchett and Wells, 2026), a necessary  
48 activity to achieve wildfire resiliency.

49 The availability of long-term (i.e., decadal-scale) satellite-based fire de-  
50 tectations at daily-sub-daily timescales and high spatial resolution ( $< 1000\text{ m}$ ),  
51 makes it possible to produce climatologies of fire activity at daily resolution.

52 Depending on whether the goal is to support operational fire management or  
53 community messaging, long-term planning and adaptation efforts to reduce  
54 fire hazard in fire-prone regions, or research activities regarding the fire envi-  
55 ronment, the region of interest may vary. A region could be jurisdictionally  
56 defined, such as a county or National Weather Service County Warning Area.  
57 It could also be a physically-defined region such as a watershed, mountain  
58 range, or pyrome. Ultimately, the spatial region selected depends on the  
59 desired application of the user.

60 This brief communication provides examples of the different perspectives  
61 offered by a pyroclimograph using four examples from three fire-prone land-  
62 scapes. First, we introduce the concept with a region experiencing distinct  
63 fire regimes (Colusa County, California). Second, we show how pyroclimo-  
64 graphs can document the progression of the Southern Great Plains fire season  
65 in real-time for an area of shared weather forecast responsibility. Third, we  
66 show how results vary across the Los Angeles County (California) region us-  
67 ing four different geographic boundaries including all or part of the county  
68 and surrounding regions. Fourth, we demonstrate how a more complete py-  
69 roclimograph can be produced at the mountain range scale by incorporating  
70 additional fire environment data by including weather and fuels information  
71 from gridded data products, weather stations, and live fuel moisture obser-  
72 vations.

## 73 **2. Data**

74 We used satellite fire detections from the Moderate Resolution Imag-  
75 ing Spectroradiometer (MODIS) onboard the Terra (2002–2025) and Aqua  
76 (2001–2025) spacecraft. Data was acquired from the NASA Fire Information  
77 for Resource Management System ([https://firms.modaps.eosdis.nasa.  
78 gov/](https://firms.modaps.eosdis.nasa.gov/)) for the period spanning 1 January 2001 to 1 April 2026. Shape-  
79 files of Colusa and Los Angeles County were acquired from the U.S. Cen-  
80 sus Bureau (<https://www2.census.gov/geo/tiger/TIGER2025/COUNTY/>).  
81 Shapefiles for the National Weather Service Los Angeles, Norman, and Amar-  
82 illo Weather Forecast Office County Warning Areas were acquired from the  
83 National Weather Service (<https://www.weather.gov/gis/CWABounds>). The  
84 boundary of the Los Angeles County Climate Assessment Region, used to  
85 support planning and adaptation efforts, was downloaded from the Califor-  
86 nia Open Data Portal ([https://data.ca.gov/dataset/ca-4th-climate-  
87 change-assessment-regions](https://data.ca.gov/dataset/ca-4th-climate-change-assessment-regions)). The Southern California Mountains/North-

ern Baja pyrome was extracted from (Short et al., 2020). Last, we used the Santa Monica Mountains (a subset of the Transverse Ranges and excluding the Palos Verdes Hills) from the Global Mountain Biodiversity Assessment Mountain Inventory version 2.0 (Snethlage et al., 2022a,b).

To more fully characterize the fire environment, we used period-of-record (January 1995–February 2026) hourly observations of 2 m air temperature, 2 m relative humidity and 6 m (20 ft) wind speed from the Malibu Hills, California Remote Automatic Weather Station (RAWS; acquired from the Western Regional Climate Center at: <https://raws.dri.edu>). Daily, gridded 4 km horizontal resolution estimates of maximum temperature, precipitation, and 100 hour dead fuel moisture spanning 1979–2025 were acquired from the gridMET product (Abatzoglou, 2013). Live fuel moisture observations data for chamise (*Adenostoma fasciculatum*) from six sites in the Santa Monica Mountains (Trippet Ranch, Laurel Canyon, Scheuren Road, Clark Motorway, Stunt Road, and Los Robles) with sampling records beginning between 2001–2006, was acquired from the Fuel Moisture Repository Webportal (<https://www.nfmdb.org/>).

### 3. Methods

All analysis was performed using Matlab (The MathWorks Inc., 2024). Shapefiles from each satellite platform were imported as arrays of fire detection latitude, longitude, fire radiative power (FRP), and time of detection. Desiring maximum detectability, we did not omit detections based on confidence values. Dates were sorted in descending order of total FRP, and cumulative FRP was calculated to estimate how many days provide 50%, 75% and 90% of the total period-of-record FRP. For individual years, cumulative FRP starting on 1 January are shown (Figure 1a). For each calendar day across all years, the total number of detections are counted and reported by a bar chart (Figure 1b); specific years of interest can be plotted separately. Cumulative FRP across each calendar day is calculated to show general fire activity seasonality (right hand y-axis of Figure 1b).

For the Santa Monica Mountains example, gridMET-based estimates of daily precipitation were extracted for a box encompassing the region. The daily mean was calculated and aggregated to monthly totals for each year. The top and bottom 5<sup>th</sup> percentiles and 50<sup>th</sup> percentile was estimated for each month to demonstrate monthly precipitation variability. The daily mean maximum temperature from gridMET was calculated and the top 5<sup>th</sup> and

124 50<sup>th</sup> percentile was calculated to provide an estimate of the typical hottest  
125 and average maximum temperatures across the year. Similarly, the mean 100  
126 hr dead fuel moisture was calculated and the top and bottom 5<sup>th</sup> percentiles  
127 and 50<sup>th</sup> percentile was estimated to provide information about the range of  
128 moisture conditions of dead fuels in the 100 hr time lag size class (woody  
129 material 2.5–7.5 cm in diameter).

130 A climatology of live fuel moisture was produced by aggregating the six  
131 sampling sites and calculating a +/-6 day moving median for each calendar  
132 day of the year following (Guirguis et al., 2025). Critically low live fuel mois-  
133 ture values as interpreted by Brown and Shelton (2025) and Dennison and  
134 Moritz (2009) provide reference indicators of elevated large fire probability.  
135 Fine and dead fuel moisture (FDFM) and probability of ignition (PIG) were  
136 calculated hourly at a steep, south aspect level with the fire based on lookup  
137 tables (National Wildfire Coordinating Group, 2025) using hourly temper-  
138 ature and relative humidity from RAWS. For each calendar day, the lowest  
139 5<sup>th</sup> percentile FDFM and highest 5<sup>th</sup> PIG are reported to highlight fuelbed  
140 receptiveness to ignition. Last, fire weather hours were estimated using the  
141 period-of-record summed daily number of hours meeting the relative humid-  
142 ity (< 10%) and sustained wind speed (> 6.7  $m s^{-1}$  (> 15 *miles hr<sup>-1</sup>*)) cri-  
143 teria for a Red Flag Warning at the National Weather Service Fire Weather  
144 Zones 369 and 370 (California Annual Operating Plan, 2025). For a Red Flag  
145 Warning to be issued, these conditions must be sustained for > 6hr. This  
146 requirement was omitted to yield a more inclusive indicator of when dry and  
147 windy conditions climatologically occur.

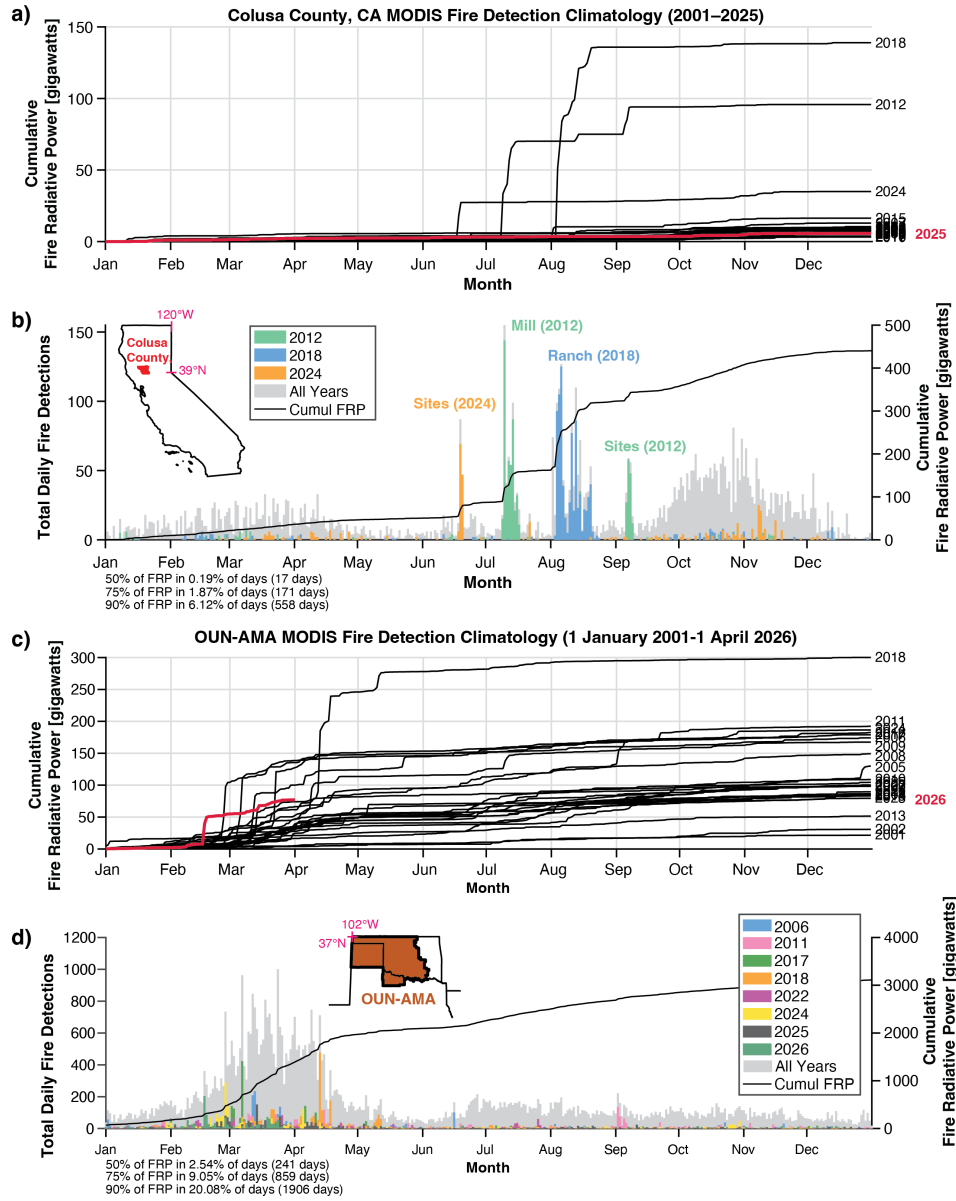


Figure 1: (a) Pyroclimograph showing daily cumulative fire radiative power for each calendar year (2001–2025; black lines; 2025 colored red) using MODIS satellite fire detections for Colusa County, California. (b) Alternative (recommended for singular use) pyroclimograph showing daily (bars; left y-axis) and cumulative (black line; right y-axis) MODIS satellite fire detections for Colusa County, California with notable fires named and colored by year. (c–d) As in (a–b) but for the Norman, Oklahoma (OUN) and Amarillo, Texas (AMA) National Weather Service County Warning Areas.

148 **4. Results**

149 *4.1. Pyroclimographs vary with fire detection input data*

150 Colusa County, CA—an agricultural community—demonstrates three dis-  
151 tinct burn seasons as evidenced by shallow increases in annual accumulations  
152 of fire radiative power (FRP) during late winter to early spring (mid-January–  
153 April), a more rapid increase during the extended summer but dominated by  
154 occasional large wildfire incidents (late June–September), and a shift back  
155 to shallow but annually consistent increases during fall (October–November;  
156 Figure 1a)). Daily detections (Figure 1b) more clearly indicate the seasonal  
157 nature of intentional burning of agricultural lands composed of orchards,  
158 vineyards and rice fields) and prescribed burning of wildlands during spring  
159 and fall as well as the short duration occasional (e.g., 2012, 2018, and 2024)  
160 but higher intensity and larger area (interpreted from the number of detec-  
161 tions) of wildfires during the peak warm season.

162 Wildfire and intentional fire occur in the Southern Great Plains through-  
163 out the year, though a peak in fire activity occurs in February following  
164 the dry winter season and terminates with the onset of the spring convec-  
165 tive season in April (Figure 1c-d). Pyroclimographs can be used to track  
166 near-real-time progression of a fire season. Following persistent drought and  
167 heavy fine fuel loading, the 2026 wildfire season started anomalously early  
168 (red line; Figure 1c) with the individual 2026 wildfire outbreak(s) placed into  
169 satellite-era climatological context in terms of timing and magnitude (Figure  
170 1d). While the annual cumulative curves allow the comparison of years and  
171 events against one another (i.e., to identify early onset of fire activity), for  
172 the remainder of the manuscript we focus on the daily bar charts and single  
173 annual accumulated FRP (e.g., Figure 1b and 1d).

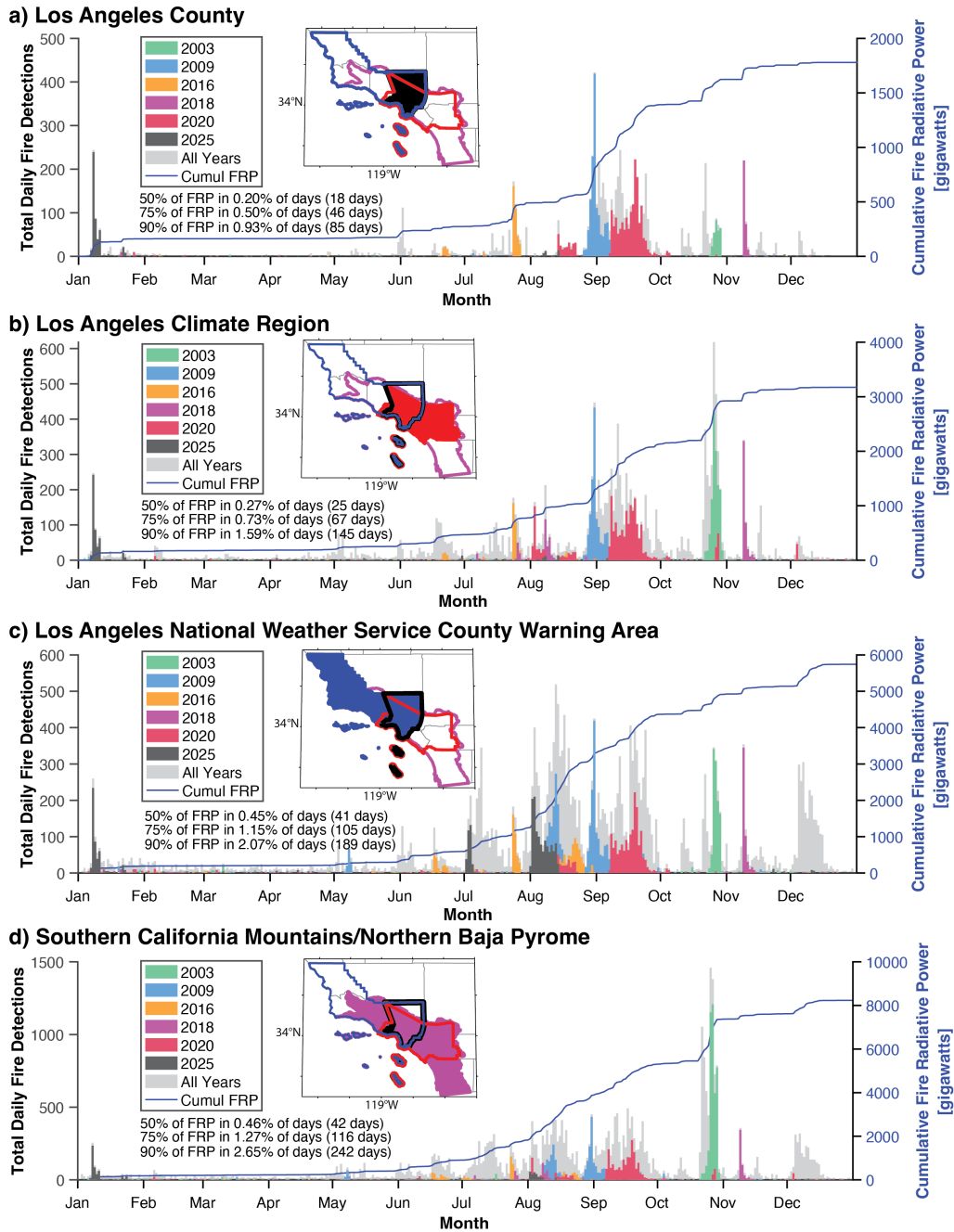


Figure 2: Pyroclimographs for (a) Los Angeles County, California, (b) the Los Angeles California Climate Assessment Region, (c) the Los Angeles National Weather Service County Warning Area, and (d) the Southern California Mountains/Northern Baja Pyrome. Each region is color filled in the associated inset map with other regions outlined.

174 *4.2. Variability across the Los Angeles region*

175 The Los Angeles region of Southern California is a densely populated fire-  
176 prone but ignition-limited landscape with extraordinary exposure of values-  
177 at-risk to wildland fire. The typical Los Angeles County fire season occurs  
178 between June to mid-November but peaks between August–September, with  
179 the anomalous nature of the January 2025 Los Angeles Fire Disaster appar-  
180 ent. (Figure 2a). The Los Angeles Climate Region (Figure 2b) follows the  
181 crest of the Transverse and Peninsular Ranges and includes Orange and parts  
182 of Riverside and San Bernardino counties. Including additional fire-prone re-  
183 gions and populated areas (i.e., ignition sources) extends the periods of peak  
184 fire activity earlier into May and includes several additional large fire events  
185 in October (2003) and November (2018).

186 The Los Angeles National Weather Service County Warning Area shifts  
187 the area of focus northwestward into San Luis Obispo and Santa Barbara  
188 counties while omitting Orange, Riverside, and San Bernardino counties  
189 (Figure 2b). This area includes more agricultural and rural areas perform-  
190 ing prescribed burning as indicated by the consistency of detections during  
191 January–May. It also encompasses more warm season fire activity result-  
192 ing from drier interior regions and elevated terrain susceptible during the  
193 Mediterranean dry season to human and lightning ignitions. Delayed on-  
194 set of winter precipitation favors December–January fires such as the 2017  
195 Thomas Fire (uncolored in Figure 2c) and the 2025 Los Angeles Fire Dis-  
196 aster. The Southern California Mountains/Northern Baja Pyrome spans  
197 interior Santa Barbara County to San Diego County (Figure 2d) and yields  
198 an extensive wildfire season from May–early January that also includes cool  
199 season prescribed burning. By including the October 2003 (green) and 2007  
200 (uncolored) San Diego County fires, other fire activity (detections and FRP)  
201 appears muted in comparison.

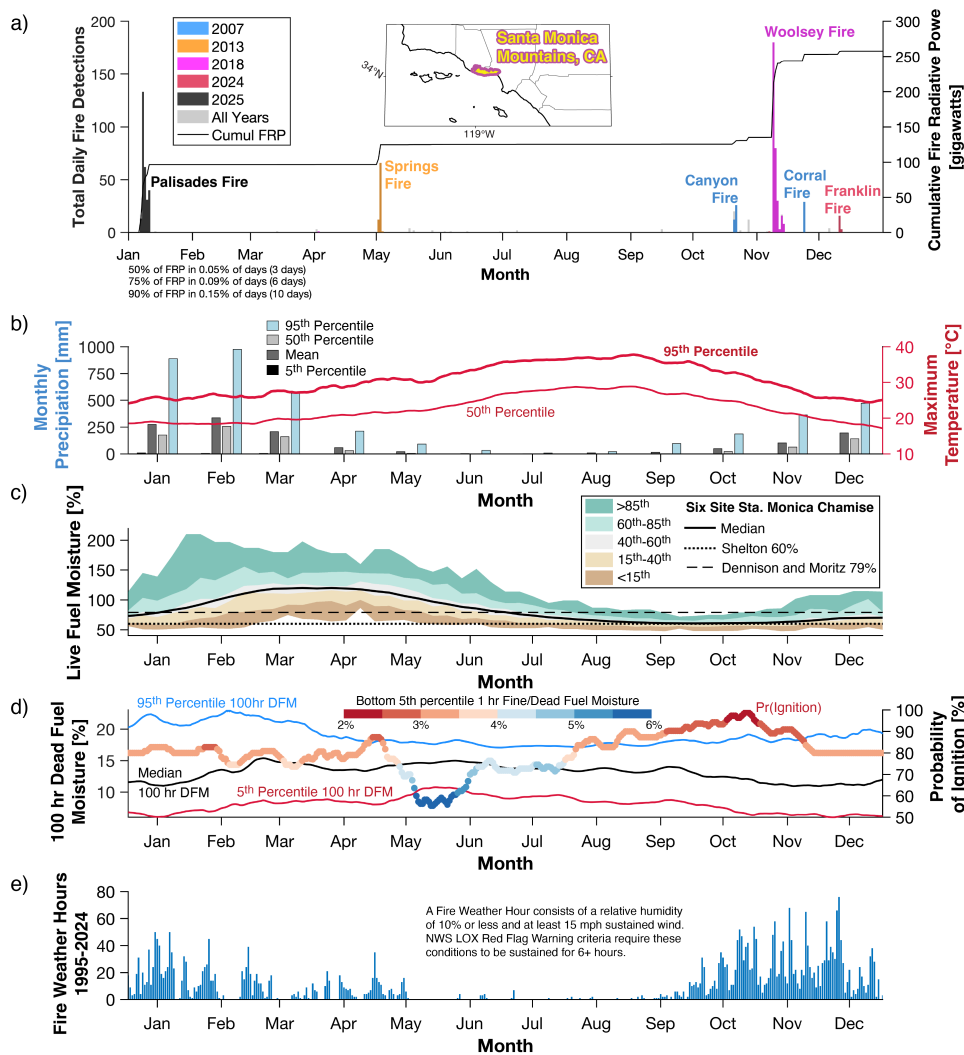


Figure 3: (a) Pyroclimograph showing daily (bars; left y-axis) and cumulative (black line; right y-axis) MODIS-based satellite fire detections for the Santa Monica Mountains of California (inset map) with notable fires named and colored. (b) Monthly mean precipitation distributions (colored bars; left y-axis) and 50<sup>th</sup> and 95<sup>th</sup> percentile maximum daily temperature (red lines; right y-axis), both calculated spanning 1979–2025 using gridMET (Abatzoglou, 2013). (c) Measured live fuel moisture for chamise (*Adenostoma fasciculatum*) across six sites. (d) Monthly mean 100-hour dead fuel moisture distributions (colored lines; left y-axis) calculated spanning 1979–2025 using gridMET. Top daily 5<sup>th</sup> percentile probability of ignition (circles) colored by the lowest 5<sup>th</sup> percentile one-hour fine and dead fuel moisture (right y-axis); both calculated from lookup tables (National Wildfire Coordinating Group, 2025) at the Malibu Hills Remote Automatic Weather Station (RAWS) for the period spanning January 1995–February 2026. (e) Total daily fire weather hours calculated from the Malibu Hills RAWS using the criteria for the National Weather Service Fire Weather Zones 369 and 370.

202 *4.3. Towards a more complete pyroclimograph*

203 Our motivation to extend the monthly-scale pyroclimograph proposed by  
204 Swetnam et al. (2011) centers on the providing a more complete picture of  
205 fire activity and the fire environment at daily timescales. The Santa Monica  
206 Mountains of Ventura and Los Angeles counties represent an ideal location to  
207 demonstrate how fire weather deviates from climatological conditions. Here,  
208 occasional, but potentially-high-impact wildfires can occur throughout the  
209 year, with 10 days contributing 90% of total FRP (Figure 3a).

210 Monthly precipitation and temperature ranges (Figure 3b) suggest why  
211 occasional fires occur despite an otherwise quiescent climate. There is a  
212 pronounced seasonal cycle of wet winters, dry summers, and variable precip-  
213 itation during spring and fall. Yet every month can be nearly completely dry,  
214 increasing fuel receptivity, and winter months can be very wet, contributing  
215 to fine fuel growth. While cool temperatures during winter–spring is followed  
216 by consistently dry summers and peak warmth in late summer–early fall, the  
217 95<sup>th</sup> percentile of cool season daily maximum temperatures can still achieve  
218 median summer temperatures. Although live fuel moistures also demonstrate  
219 a seasonal cycle driven by plant phenology and resource availability, extended  
220 drought can maintain critically low moistures (Figure 3c).

221 The 100dfm (Figure 3d) represents the upper bound of standing dead  
222 vegetation size classes in chaparral-dominated ecosystems. The most pro-  
223 nounced seasonal variation of 100dfm occurs between October–February,  
224 with the smaller range between May–August. Values from October to Jan-  
225 uary approach 5% during drought and exceed 20% during prolonged wet/cool  
226 conditions. The median ranges between 11–14% throughout the year. The  
227 most receptive FDFM highlights additional weather-driven impacts. While  
228 it indicates much of the year can have PIG exceed 70% on ‘worst case slopes’,  
229 it also reflects the signal of marine stratus in May–June. FDFM shows two  
230 relative maxima (*gt90%*) of fuelbed receptivity, a subtle peak prior to spring  
231 marine layer onset and the fall hot and dry season in Southern California.

232 Until now, the pyroclimograph has focused on the ignition component of  
233 the fire environment. Inclusion of wind, and particularly wind associated with  
234 low relative humidity, incorporates the spread component. Using the Using  
235 the relative humidity and wind criteria for Red Flag Warnings but omit-  
236 ting the wind duration constraint, dry and windy conditions relatively rarely  
237 occur from May–September before increasing and reaching peak frequency  
238 during October–November (Figure 3e). They decline through the winter be-  
239 fore a secondary peak between March–April. Just as the FDFM highlighted

240 the marine stratus season, fire weather hours highlight two regional critical  
241 fire weather patterns affecting the Santa Monicas: the fall–winter Santa Ana  
242 season followed by the spring Sundowner Winds (Hatchett et al., 2018).

## 243 **5. Discussion**

244 Daily-scale pyroclimographs, using satellite data, allows a more granular  
245 temporal and spatially-explicit perspective than historic fire perimeters that  
246 offer only singular dates of discovery and containment (Swetnam et al., 2011)  
247 or monthly aggregations of satellite data (Giglio et al., 2009; Sablan et al.,  
248 2024). It also allows for agricultural or prescribed burns to be included,  
249 assuming burning occurred during satellite overflight, without acquiring burn  
250 permit data (Sweeney et al., 2025; Worsnop et al., in revision). The utility of  
251 pyroclimographs rests in their use as both a training tool to understand recent  
252 fire history and as a tool to document and contextualize the evolution of a fire  
253 season or identify periods of good fire weather (Hatchett and Wells, 2026).  
254 Importantly, our approach visualizes a minimum of fire activity: satellites do  
255 not capture all pixels burning at all times as wildland fire progresses across  
256 the landscape and cannot capture fires that do not produce a detectable  
257 heat signature. An upcoming challenge for data continuity will be merging  
258 MODIS detection climatologies with other data sources such as the Visible  
259 Infrared Imaging Radiometer Suite (VIIRS) as the MODIS mission undergoes  
260 decommissioning.

261 Reporting climatological mean conditions likely underestimates the po-  
262 tential for fire activity, which may only require several hours to yield favorable  
263 conditions for ignition and rapid spread. It also prevents clear identification  
264 of the frequency, timing, magnitude, and duration of anomalous conditions  
265 favoring wildland fire. Because many fire-prone regions are characterized by  
266 variability of environmental conditions across intraseasonal, interseasonal,  
267 and interannual timescales, inclusion of fire weather variability, as done here,  
268 only estimate the first-order potential for fire. Identifying the specific condi-  
269 tions associated with burning will aid the identification of the atmospheric  
270 processes driving them, improving their predictability and thus community  
271 preparation. Subsequent iterations of pyroclimographs will include local con-  
272 ditions extracted on the day of burning to place these into climatological  
273 context.

## 274 **6. Closing Remarks**

275 We revisited the concept of pyroclimographs as simple visualizations  
276 leveraging satellite fire detections to demonstrate a facet of pyrogeography:  
277 the “where of fire when” to understand “the why of fire”. Providing a daily  
278 perspective of wildland fire activity, pyroclimographs contextualize a region’s  
279 satellite-era fire history and support the interpretation of past fire events, es-  
280 pecially when complemented with fire environment data. With no additional  
281 information, a pyroclimograph indicates when fire activity has not (yet) been  
282 observed, when fire activity may be common but intentional (i.e., prescribed  
283 and agricultural burning; Worsnop et al. in revision), when wildfire activity  
284 is most frequent and intense, or when wildfires can be managed for resource  
285 benefit. By including fire environment-related data and its variability, a pic-  
286 ture emerges of why certain seasons typically do or do not have increased fire  
287 activity and why anomalous events occurred. The simplicity of pyroclimo-  
288 graphs is intentional; it is our aim that they can be used not just for research  
289 or tracking purposes but also educational and training purposes for broad  
290 audiences to understand the relationship of wildland fire to a place.

## 291 **7. Code Availability**

292 Matlab code to produce pyroclimographs is available upon request; it is  
293 slated to be released publicly in mid-2026.

## 294 **8. Acknowledgements**

### 295 **References**

- 296 Abatzoglou, J.T., 2013. Development of gridded surface meteorological data  
297 for ecological applications and modelling. *International Journal of Clima-*  
298 *tology* 33, 121–131. doi:<https://doi.org/10.1002/joc.3413>.
- 299 Al-Yaari, A., Condom, T., Junquas, C., Rabatel, A., Ramseyer, V., Sicart,  
300 J.E., Masiokas, M., Cauvy-Fraunié, S., Dangles, O., 2023. Climate vari-  
301 ability and glacier evolution at selected sites across the world: Past trends  
302 and future projections. *Earth’s Future* 11, e2023EF003618. doi:<https://doi.org/10.1029/2023EF003618>.
- 304 Brown, T., Shelton, J., 2025. Confluence of fire and people. *Nature Sustain-*  
305 *ability* 8, 329–330. doi:10.1038/s41893-025-01541-9.

- 306 California Annual Operating Plan, 2025. California Annual Operating Plan  
307 2025. [https://www.weather.gov/media/wrh/cafw/2025\\_CA\\_FIRE\\_AOP.](https://www.weather.gov/media/wrh/cafw/2025_CA_FIRE_AOP.pdf)  
308 [pdf](https://www.weather.gov/media/wrh/cafw/2025_CA_FIRE_AOP.pdf).
- 309 Dennison, P.E., Moritz, M.A., 2009. Critical live fuel moisture in cha-  
310 parral ecosystems: a threshold for fire activity and its relationship to  
311 antecedent precipitation. *International Journal of Wildland Fire* 18, 1021–  
312 1027. doi:10.1071/WF08055.
- 313 Giglio, L., Loboda, T., Roy, D.P., Quayle, B., Justice, C.O., 2009. An active-  
314 fire based burned area mapping algorithm for the modis sensor. *Remote*  
315 *Sensing of Environment* 113, 408–420. doi:[https://doi.org/10.1016/j.](https://doi.org/10.1016/j.rse.2008.10.006)  
316 [rse.2008.10.006](https://doi.org/10.1016/j.rse.2008.10.006).
- 317 Guirguis, K., Hatchett, B., Clemesha, R., Aguilera, R., Gershunov, A.,  
318 Campbell, I., Cayan, D., Merrifield, M., 2025. Compound atmospheric  
319 drivers of the catastrophic 2025 los angeles urban firestorm. *npj Natural*  
320 *Hazards* 2, 103. doi:10.1038/s44304-025-00155-7.
- 321 Hatchett, B.J., Smith, C.M., Nauslar, N.J., Kaplan, M.L., 2018. Brief com-  
322 munication: Synoptic-scale differences between sundowner and santa ana  
323 wind regimes in the santa ynez mountains, california. *Natural Hazards and*  
324 *Earth System Sciences* 18, 419–427. doi:10.5194/nhess-18-419-2018.
- 325 Hatchett, B.J., Wells, E.M., 2026. Good fire weather. *EarthArXiv Preprint*  
326 doi:<https://doi.org/10.31223/X54435>.
- 327 Lasantha, V., Oki, T., Tokuda, D., 2022. Data-driven versus köppen–geiger  
328 systems of climate classification. *Advances in Meteorology* 2022, 3581299.  
329 doi:<https://doi.org/10.1155/2022/3581299>.
- 330 National Wildfire Coordinating Group, 2025. Fire Behavior Field Reference  
331 Guide, PMS 437. URL: <https://www.nwcg.gov/publications/pms437>.  
332 Last Accessed: 2026-02-04.
- 333 Sablan, O., Ford, B., Gargulinski, E., Hammer, M.S., Henery, G., Kondra-  
334 gunta, S., Martin, R.V., Rosen, Z., Slater, K., van Donkelaar, A., Zhang,  
335 H., Soja, A.J., Magzamen, S., Pierce, J.R., Fischer, E.V., 2024. Quan-  
336 tifying prescribed-fire smoke exposure using low-cost sensors and satel-  
337 lites: Springtime burning in eastern kansas. *GeoHealth* 8, e2023GH000982.  
338 doi:<https://doi.org/10.1029/2023GH000982>.

- 339 Senande-Rivera, M., Insua-Costa, D., Miguez-Macho, G., 2022. Spatial and  
340 temporal expansion of global wildland fire activity in response to climate  
341 change. *Nature Communications* 13, 1208. doi:10.1038/s41467-022-  
342 28835-2.
- 343 Short, K.C., Grenfell, I.C., Riley, K.L., Vogler, K.C., 2020. Pyromes of the  
344 conterminous united states. Fort Collins, CO: Forest Service Research  
345 Data Archive. doi:<https://doi.org/10.2737/RDS-2020-0020>.
- 346 Snethlage, M., Geschke, J., Spehn, E., Ranipeta, A., Yoccoz, N., Körner,  
347 C., Jetz, W., Fischer, M., Urbach, D., 2022a. Gmba mountain inventory  
348 v2. URL: <https://earthenv.org/mountains>, doi:10.48601/EARTHENV-  
349 T9K2-1407.
- 350 Snethlage, M.A., Geschke, J., Ranipeta, A., Jetz, W., Yoccoz, N.G., Körner,  
351 C., Spehn, E.M., Fischer, M., Urbach, D., 2022b. A hierarchical inventory  
352 of the world's mountains for global comparative mountain science. *Scien-  
353 tific Data* 9, 149. URL: [https://doi.org/10.1038/s41597-022-01256-](https://doi.org/10.1038/s41597-022-01256-y)  
354 [y](https://doi.org/10.1038/s41597-022-01256-y), doi:10.1038/s41597-022-01256-y.
- 355 Sweeney, B., Jolly, W.M., Freeborn, P.H., Ochocki, C., 2025. ClassiFiRxe:  
356 a data-driven tool to support prescribed fire planning and implemen-  
357 tation. Preprint submitted to SSRN doi:[http://dx.doi.org/10.2139/](http://dx.doi.org/10.2139/ssrn.5846214)  
358 [ssrn.5846214](http://dx.doi.org/10.2139/ssrn.5846214).
- 359 Swetnam, T.W., Falk, D.A., Sutherland, E.K., Brown, P.M., Brown, T.J.,  
360 2011. Final report, 2011: Fire and climate synthesis (facs) project, jfsp  
361 09-2-01-10. [https://www.researchgate.net/publication/292610619\\_](https://www.researchgate.net/publication/292610619_Final_Report_2011_Fire_and_Climate_Synthesis_FACS_Project_JFSP_09-2-01-10)  
362 [Final\\_Report\\_2011\\_Fire\\_and\\_Climate\\_Synthesis\\_FACS\\_Project\\_](https://www.researchgate.net/publication/292610619_Final_Report_2011_Fire_and_Climate_Synthesis_FACS_Project_JFSP_09-2-01-10)  
363 [JFSP\\_09-2-01-10](https://www.researchgate.net/publication/292610619_Final_Report_2011_Fire_and_Climate_Synthesis_FACS_Project_JFSP_09-2-01-10).
- 364 The MathWorks Inc., 2024. Matlab version: 24.1.0 (r2024a). URL: [https:](https://www.mathworks.com)  
365 [//www.mathworks.com](https://www.mathworks.com).
- 366 Worsnop, R.P., Hoell, A., B.J., H., T.B., C., Breeden, M.L., Zach Tolby, Z.,  
367 Short, K.C., Hobbins, M., in revision. Characterizing windows of opportu-  
368 nity for prescribed pile and broadcast burning in northern california. *Fire*  
369 *Ecology* .